SOURCE SIZE AND EMITTANCE MEASUREMENTS FOR LOW-EMITTANCE LIGHT SOURCES

Xianbo Shi, Nazanin Samadi, Les Dallin, Dean Chapman

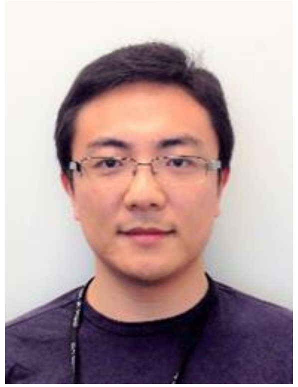

Advanced Photon Source

Paul Scherrer Institut
University of Saskatchewan
Canadian Light Source

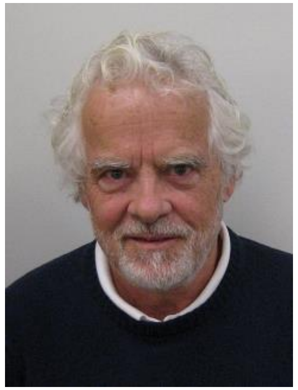

Canadian Light Source

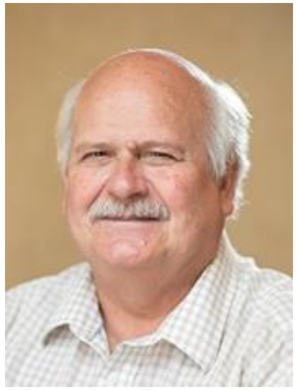

University of Saskatchewan
Canadian Light Source

IBIC 2020, Sep. 2020

Motivation

- New generation light sources with low emittance
  - High degree of coherence: coherent diffraction imaging, ptychography, XPCS etc.
  - Small beam: nano-focusing
  - High flux density
- MBA Lattice

$$\varepsilon \propto \frac{E^2}{(N_s N_d)^3}$$

$$\varepsilon_y \propto \sigma_y \sigma_y'$$

E: electron beam energy
N_s: number of sectors in the ring
N_d: number of dipoles per sector
σ: electron source size
σ': electron source divergence

- Source size and beam stability measurements are challenging and important

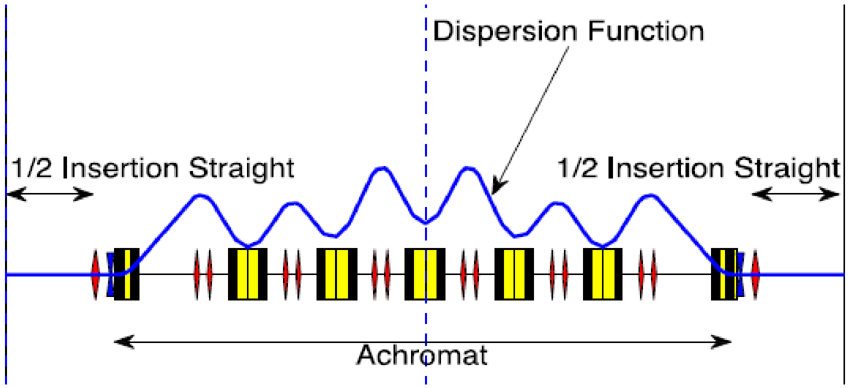

Robert Hettel IPAC14

	APS-U BM	SLS-2 BM	CLS-2 BM
σ_x (µm)	10.9	8	8.9
σ_x' (µrad)	20.6	28	7.7
σ_y (µm)	4.4	7	3.9
σ_y' (µrad)	4.4	1	0.8

Methods of measuring the source size

Imaging-based methods

- Pinhole imaging
- Coded aperture
- Compound refractive lenses
- Fresnel zone plates
- Kirkpatrick-Baez mirrors
- π polarization

Interference-based methods

- Double-slit interferometry
- Grating interferometry
- X-ray (multi/lens) interferometry
- π polarization with diffraction obstacle

Theoretical study

- N. Samadi, X. Shi, L. Dallin, and D. Chapman, “Source size measurement options for low-emittance light sources” Phys. Rev. Accel. Beams 23, 024801 (2020).
- N. Samadi presentation at IPAC20

Experimental study

- X. Shi, N. Samadi, L. Dallin, L. Assoufid, and D. Chapman, “Experimental comparison and calibration of three methods to measure electron source properties for synchrotron radiation,” (2020) to be submitted.

Something different: ps-BPM system

- **N. Samadi, “A real time phase space beam size and divergence monitor for synchrotron radiation” (PhD dissertation, University of Saskatchewan, 2019).**
- N. Samadi, X. Shi, L. Dallin, and D. Chapman, Phys. Rev. Accel. Beams 23, 024801 (2020).
- N. Samadi, X. Shi, L. Dallin, and D. Chapman, Phys. Rev. Accel. Beams 22, 122802 (2019).
- N. Samadi, X. Shi, and D. Chapman, J. Synchrotron Radiat. 26, 1863 (2019).
- N. Samadi, X. Shi, L. Dallin, and D. Chapman, J. Synchrotron Radiat. 26, 1213 (2019).
- N. Samadi, X. Shi, L. Dallin, and D. Chapman, Proc. 10th Int. Part. Accel. Conf. FRXXRLS3, 4376 (2019).
- N. Samadi, L. Dallin, and D. Chapman, Proc. IBIC2018 186 (2018).
- N. Samadi, B. Bassey, M. Martinson, G. Belev, L. Dallin, M. De Jong, and D. Chapman, J. Synchrotron Radiat. 22, 946 (2015).

Pinhole Imaging

- $\Sigma^2 = (M\sigma_y)^2 + \sigma_{\text{pinhole}}^2 + \sigma_{\text{detector}}^2$
- Minimize $\frac{\sigma_{\text{pinhole}}}{M\sigma_y}$
- Method 1: Analytical
  - $\sigma_{\text{pinhole}}^2 = \sigma_{\text{geo}}^2 + \sigma_{\text{diff}}^2$
    with $\sigma_{\text{geo}} = \frac{a}{2\sqrt{3}} \frac{(p+q)}{p}$, $\sigma_{\text{diff}} = \frac{0.886}{2.355} \frac{\lambda q}{a}$
  - $\left(\frac{\sigma_{\text{pinhole}}}{M\sigma_y}\right)_{\text{min}} = \frac{1}{\sigma_y}\sqrt{0.217\lambda\left(p + \frac{p^2}{q}\right)}$
- Method 2: Near field (NF) propagation
  - $I_s(y) = \varepsilon(y) \cdot \varepsilon^*(y)$
  - $\varepsilon(y) = \frac{1}{i\lambda q}\int_{-a/2}^{a/2} \varepsilon_0(y_0) \exp\left[\frac{i\pi}{\lambda q}(y - y_0)^2\right] dy_0$
  - $I_G = I_s(y) \otimes \left[\exp\left(-\frac{y^2 p^2}{2\sigma_y^2 q^2}\right)\right]$

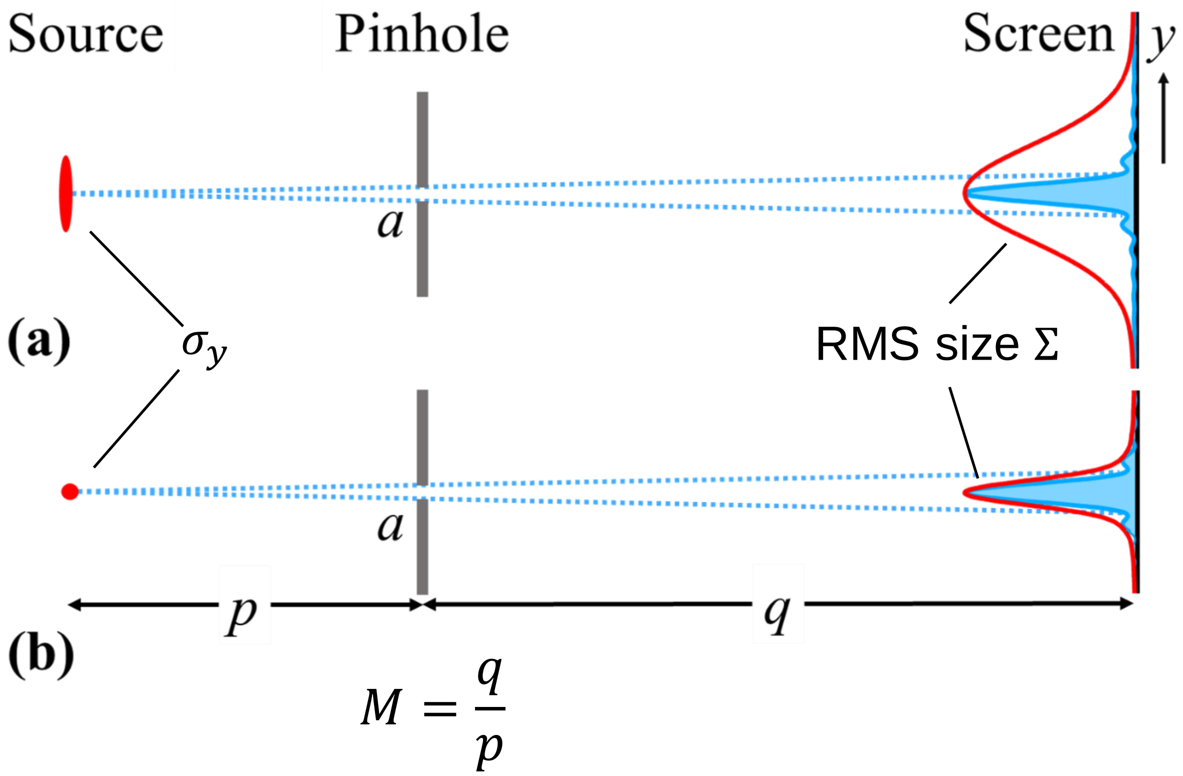

N. Samadi, X. Shi, L. Dallin, and D. Chapman, Phys. Rev. Accel. Beams 23, 024801 (2020).

Pinhole Imaging: optimization

- $\Sigma^2 = (M\sigma_y)^2 + \sigma_{\text{pinhole}}^2 + \sigma_{\text{detector}}^2$
- Minimize $\dfrac{\sigma_{\text{pinhole}}}{M\sigma_y}$
- Method 1: Analytical
  - $\sigma_{\text{pinhole}}^2 = \sigma_{\text{geo}}^2 + \sigma_{\text{diff}}^2$
    with $\sigma_{\text{geo}} = \dfrac{a}{2\sqrt{3}}\dfrac{(p+q)}{p}$, $\sigma_{\text{diff}} = \dfrac{0.886}{2.355}\dfrac{\lambda q}{a}$
  - $\left(\dfrac{\sigma_{\text{pinhole}}}{M\sigma_y}\right)_{\min} = \dfrac{1}{\sigma_y}\sqrt{0.217\lambda\left(p + \dfrac{p^2}{q}\right)}$
- Method 2: Near field (NF) propagation
  - $I_s(y) = \varepsilon(y)\cdot\varepsilon^*(y)$
  - $\varepsilon(y) = \dfrac{1}{i\lambda q}\int_{-a/2}^{a/2}\varepsilon_0(y_0)\exp\left[\dfrac{i\pi}{\lambda q}(y-y_0)^2\right]dy_0$
  - $I_G = I_s(y)\otimes\left[\exp\left(-\dfrac{y^2p^2}{2\sigma_y^2q^2}\right)\right]$

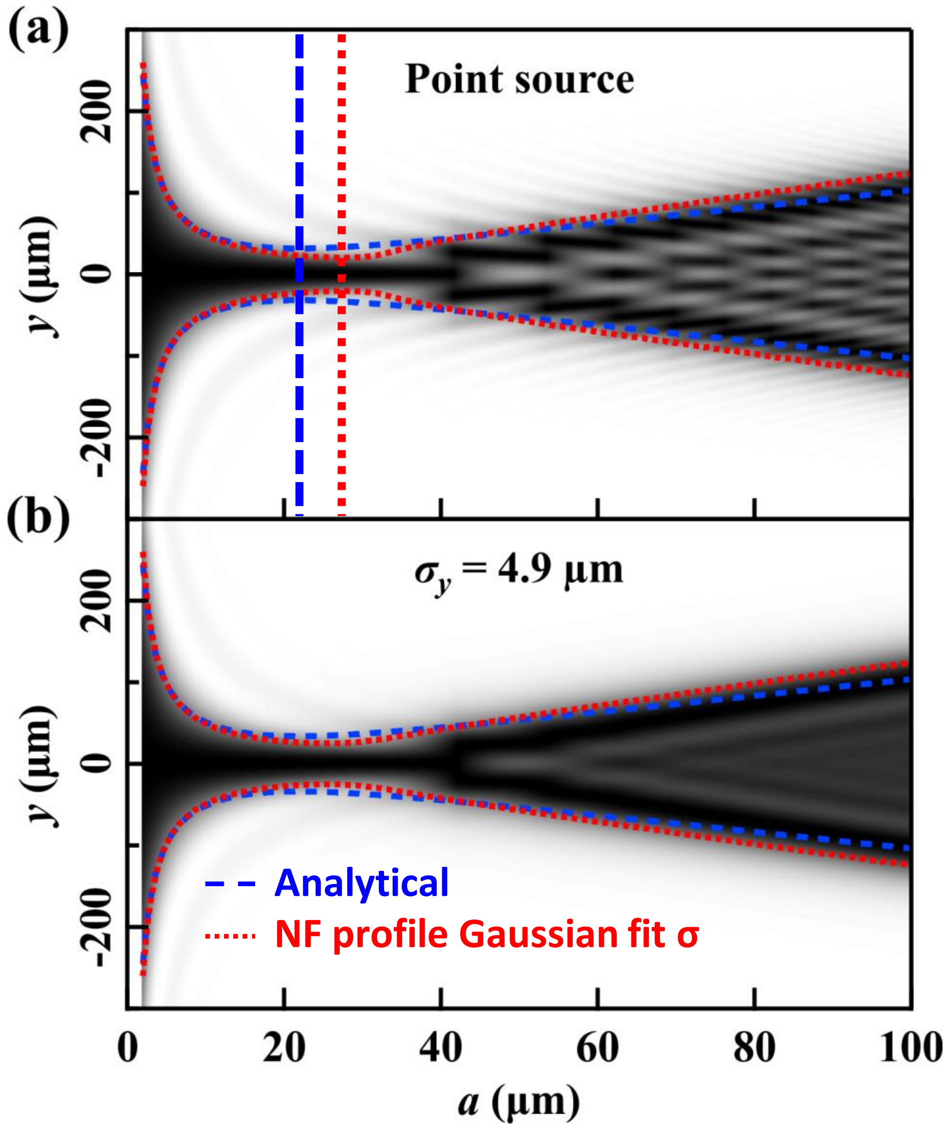

λ = 0.827 Å (photon energy, E = 15 keV)
p = 6.6 m, q = 13.4 m, APS-U M3 source

N. Samadi, X. Shi, L. Dallin, and D. Chapman, Phys. Rev. Accel. Beams 23, 024801 (2020).

Pinhole Imaging: limitation

- Optimized aperture size for different source sizes
  - Limited resolution ➡ difficult to measure source sizes < 10 micron

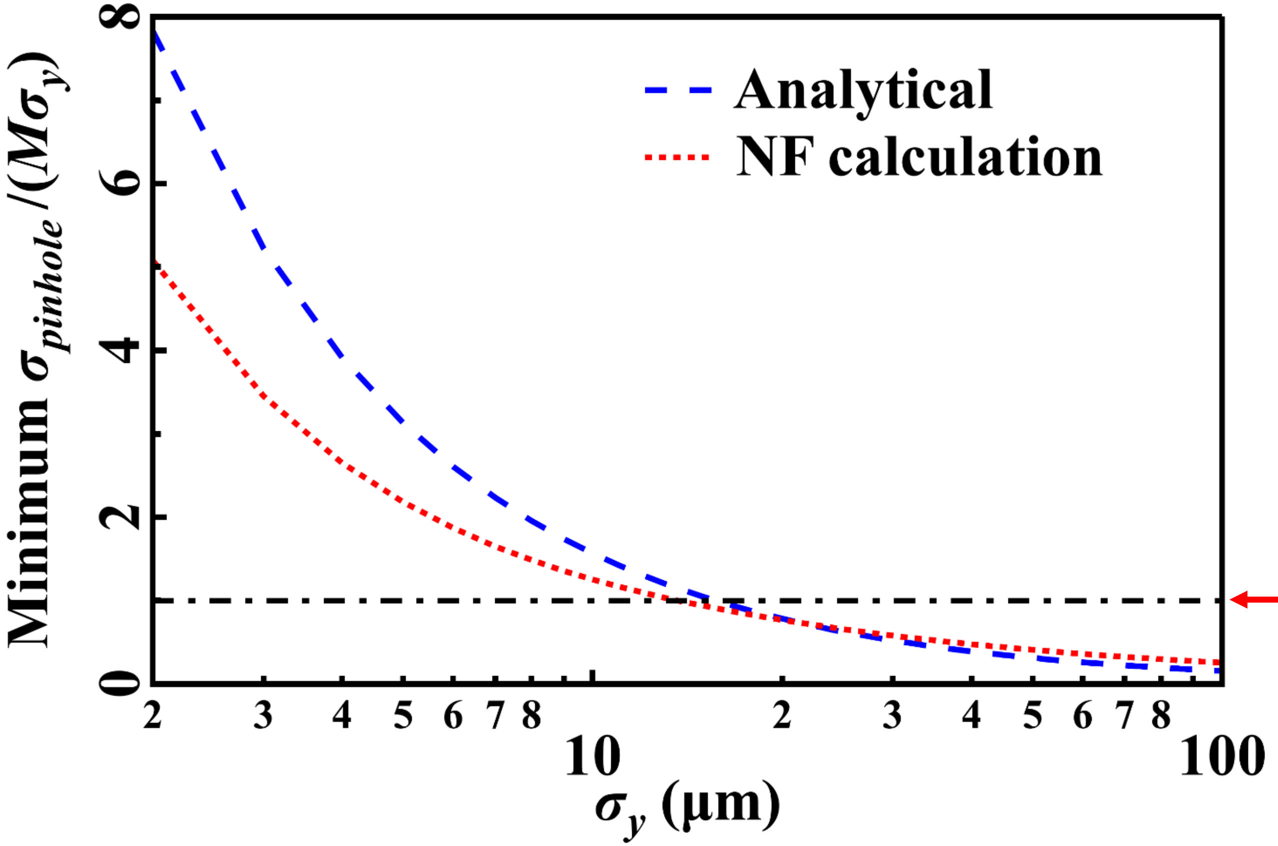

$$\left(\frac{\sigma_{\text{pinhole}}}{M\sigma_y}\right)_{\text{min}} = 1$$

N. Samadi, X. Shi, L. Dallin, and D. Chapman, Phys. Rev. Accel. Beams 23, 024801 (2020).

Pinhole Imaging: summary

	Pinhole Imaging
Optical setup	Simple, aberration free
Measurement directions	All
Fast measurement	Yes, white beam
Resolution	Limited to >10 µm
High-resolution detector	Yes
Optics fabrication	Hard
Information	Size and position

Double-Slit Interferometry

- $I = 2I_0 \mathrm{sinc}^2\left(\frac{\pi a}{\lambda q} y\right)\left[1 + V\cos\left(\frac{2\pi d}{\lambda q} y\right)\right]$
- Gaussian source

$$\sigma_y = \frac{\lambda p}{\pi d}\sqrt{\frac{1}{2}\ln\frac{1}{V}} \Rightarrow \frac{d\sigma_y}{\sigma_y} = \frac{|dV|}{2V\ln\frac{1}{V}}$$

- Minimize the source size sensitivity $\frac{d\sigma_y}{\sigma_y}$

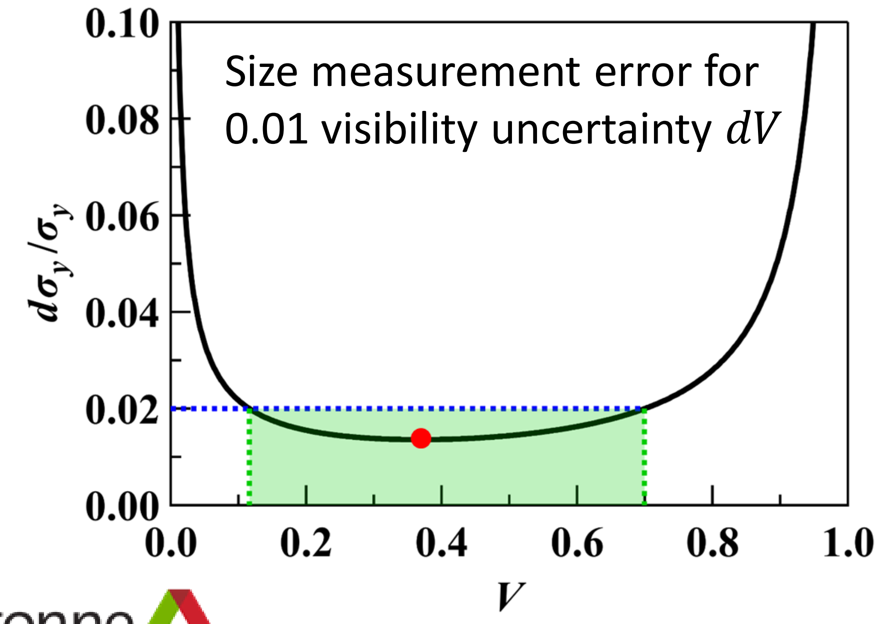

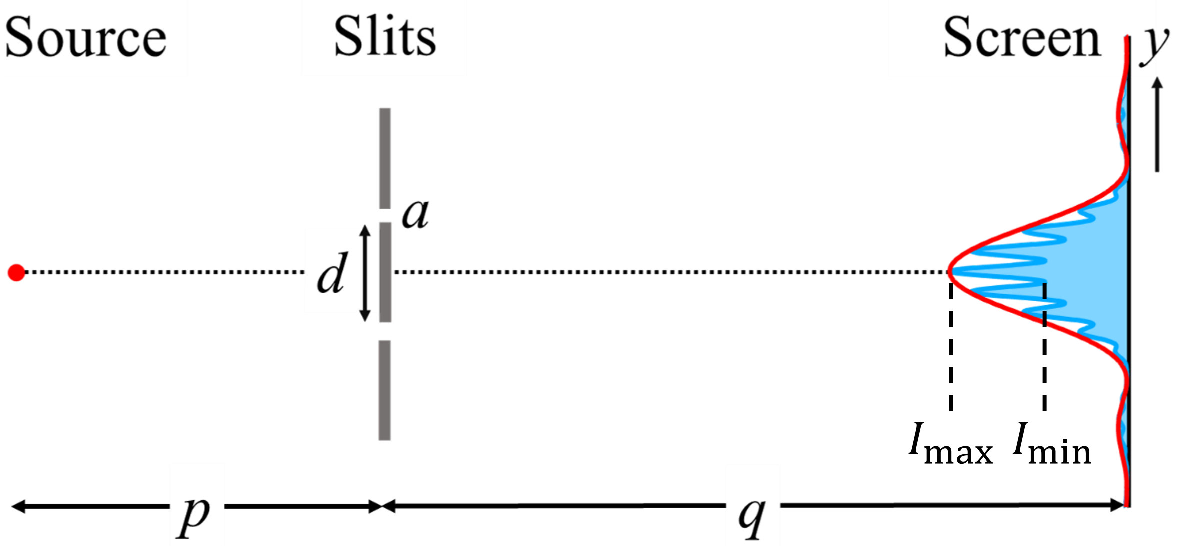

$$V = \frac{I_{max} - I_{min}}{I_{max} + I_{min}}$$

- Minimum $d\sigma_y/\sigma_y$ at $V = 0.37$
- To ensure 2% sensitivity of source size measurement, the required visibility range $0.12 < V < 0.70$

N. Samadi, X. Shi, L. Dallin, and D. Chapman, Phys. Rev. Accel. Beams 23, 024801 (2020).

Double-Slit Interferometry: optimization

- **Slit separation d study**
  - Optimized at size (V= 0.37) $\sigma_y = 0.225\frac{\lambda p}{d}$
  - Detectable size range with at least 2% sensitivity (0.12<V<0.70): $0.13(\frac{\lambda p}{d})<\sigma_y<0.33(\frac{\lambda p}{d})$

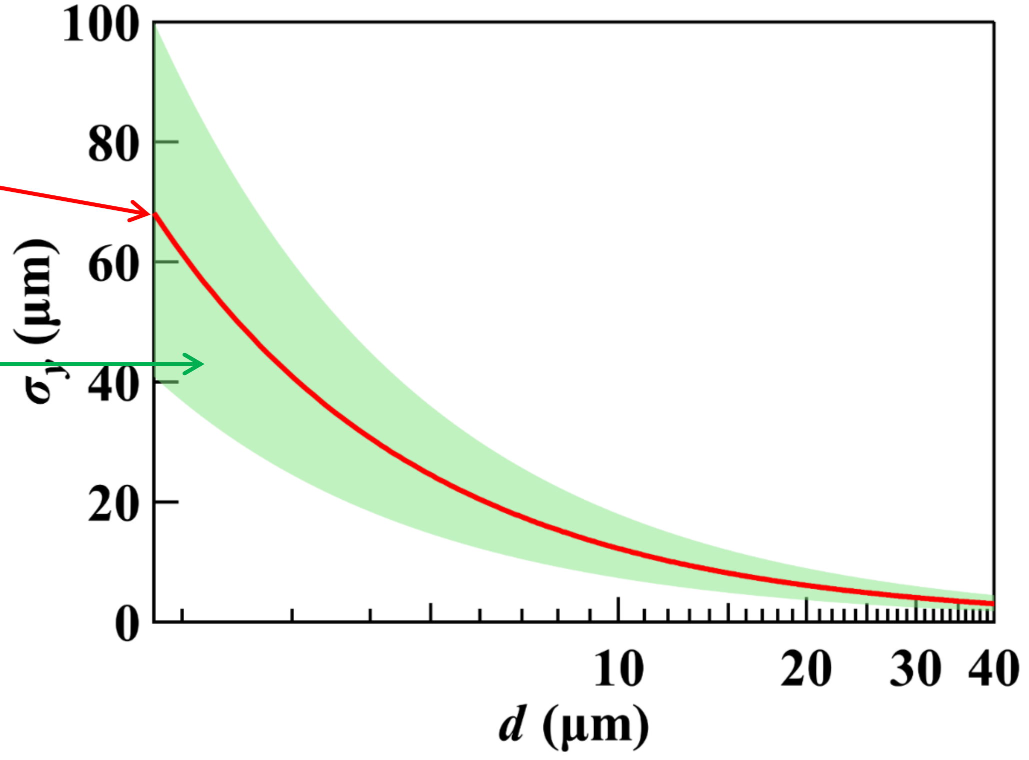

- **Slit size a study**

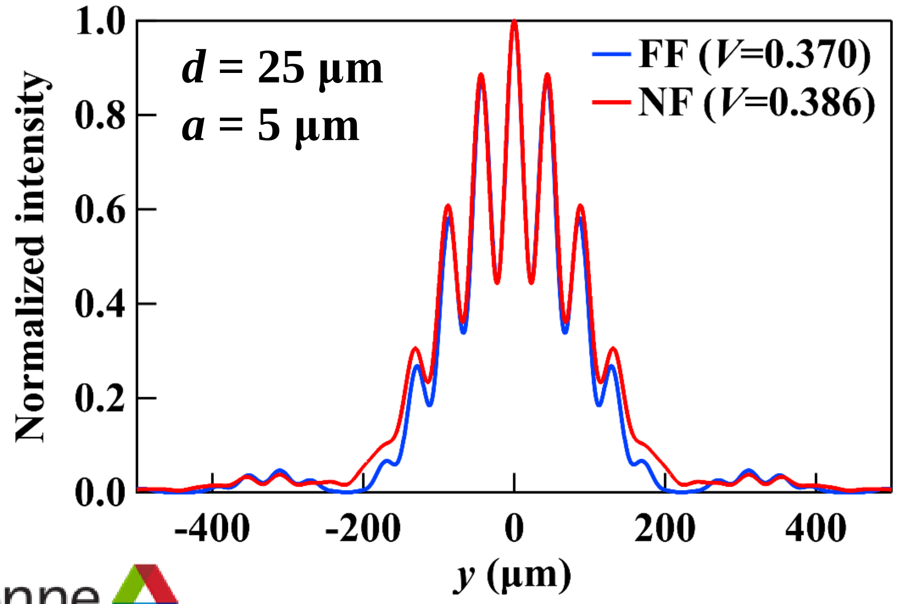

- a needs to be small enough (<d/5) to ensure far-field approximation is valid
- Larger a, higher flux density

N. Samadi, X. Shi, L. Dallin, and D. Chapman, Phys. Rev. Accel. Beams 23, 024801 (2020).

Double-Slit Interferometry: summary

	Pinhole Imaging	Double Slit Interferometry
Optical setup	Simple, aberration free	Require monochromator
Measurement directions	All	1-D
Fast measurement	Yes, white beam	No
Resolution	Limited to >10 μm	Highest
High-resolution detector	Yes	Yes
Optics fabrication	Hard	Hard
Information	Size and position	Size only

ps-BPM

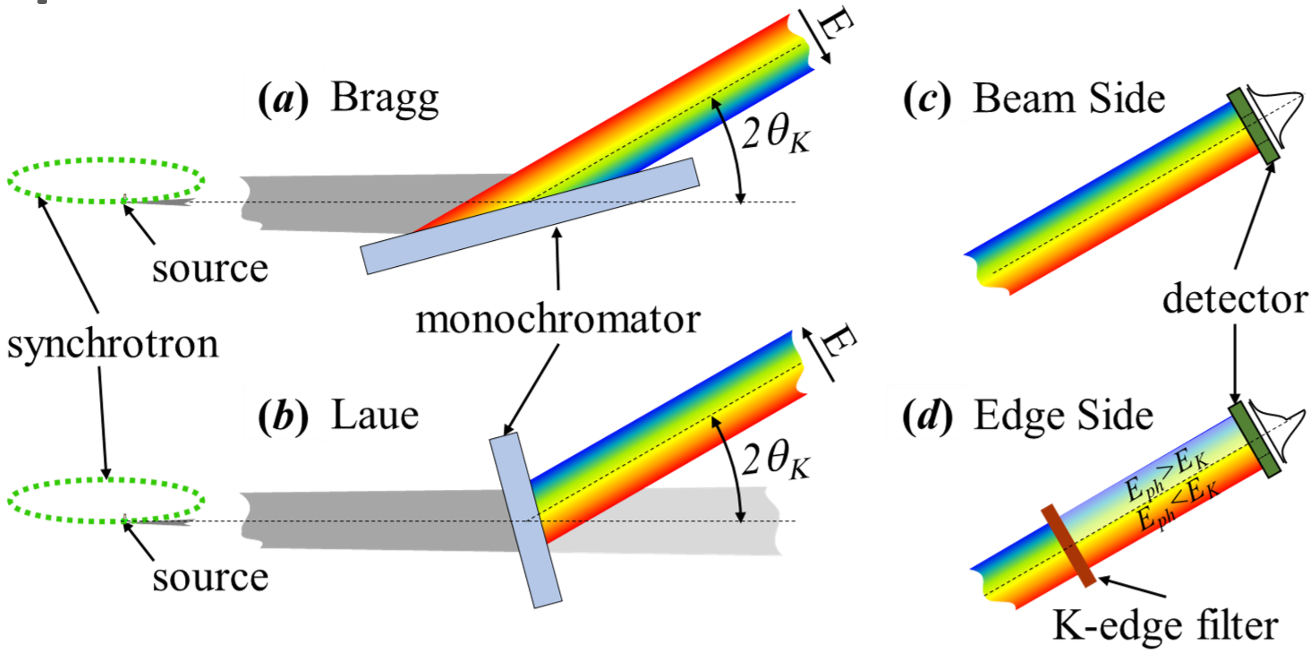

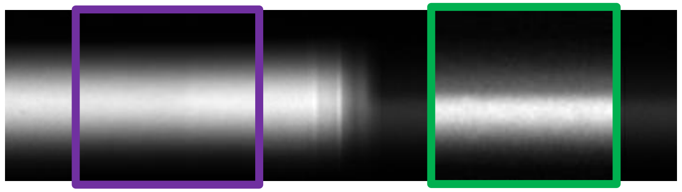

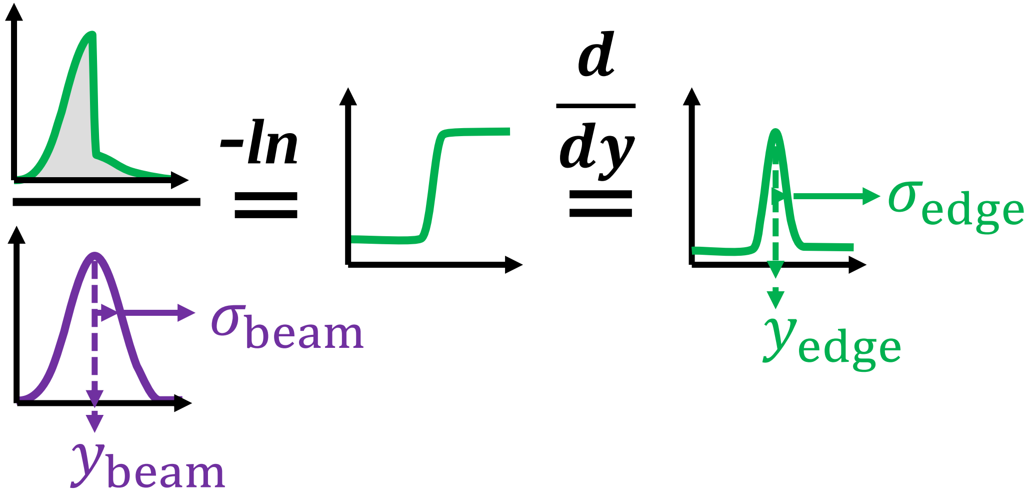

$$y = y_{\text{edge}}$$

$$\sigma_y = \sqrt{\sigma_{\text{edge}}^2 - (D\sigma_{y'_{K-\text{edge}}})^2 - (D\sigma_{y'_{\text{mono}}})^2}$$

$$y' = \frac{y_{\text{beam}} - y_{\text{edge}}}{D}$$

$$\sigma_{y'} = \frac{1}{D}\sqrt{\sigma_{\text{beam}}^2 - \sigma_y^2 - (D\sigma_{y'_{\text{Ph}}})^2}$$

N. Samadi, X. Shi, L. Dallin, and D. Chapman, J. Synchrotron Radiat. 26, 1213 (2019).

PAUL SCHERRER INSTITUT

ps-BPM: optimization

- $\sigma_{IRF} = D\sigma_{y'_{\text{total}}} = D\sqrt{\sigma^2_{y'_{\text{mono}}} + \sigma^2_{y'_{K-\text{edge}}}}$
- Small source-to-detector distance, *D*
- Effect dominated by the angular projected *K*-edge width

$$\sigma_{y'_{K-\text{edge}}} = \frac{\tan\theta_K}{E_K}\sigma_{E_{K-\text{edge}}}$$

  - Small $\sigma_{E_{K-\text{edge}}}$
  - Large E_K
  - Small θ_K (low reflection index)

Shadow simulation of ps-BPM for APS-U Source

- Si (111) single Bragg, Barium K-edge (37.441 keV)
- *D* = 10 m, detector resolution 10 µm

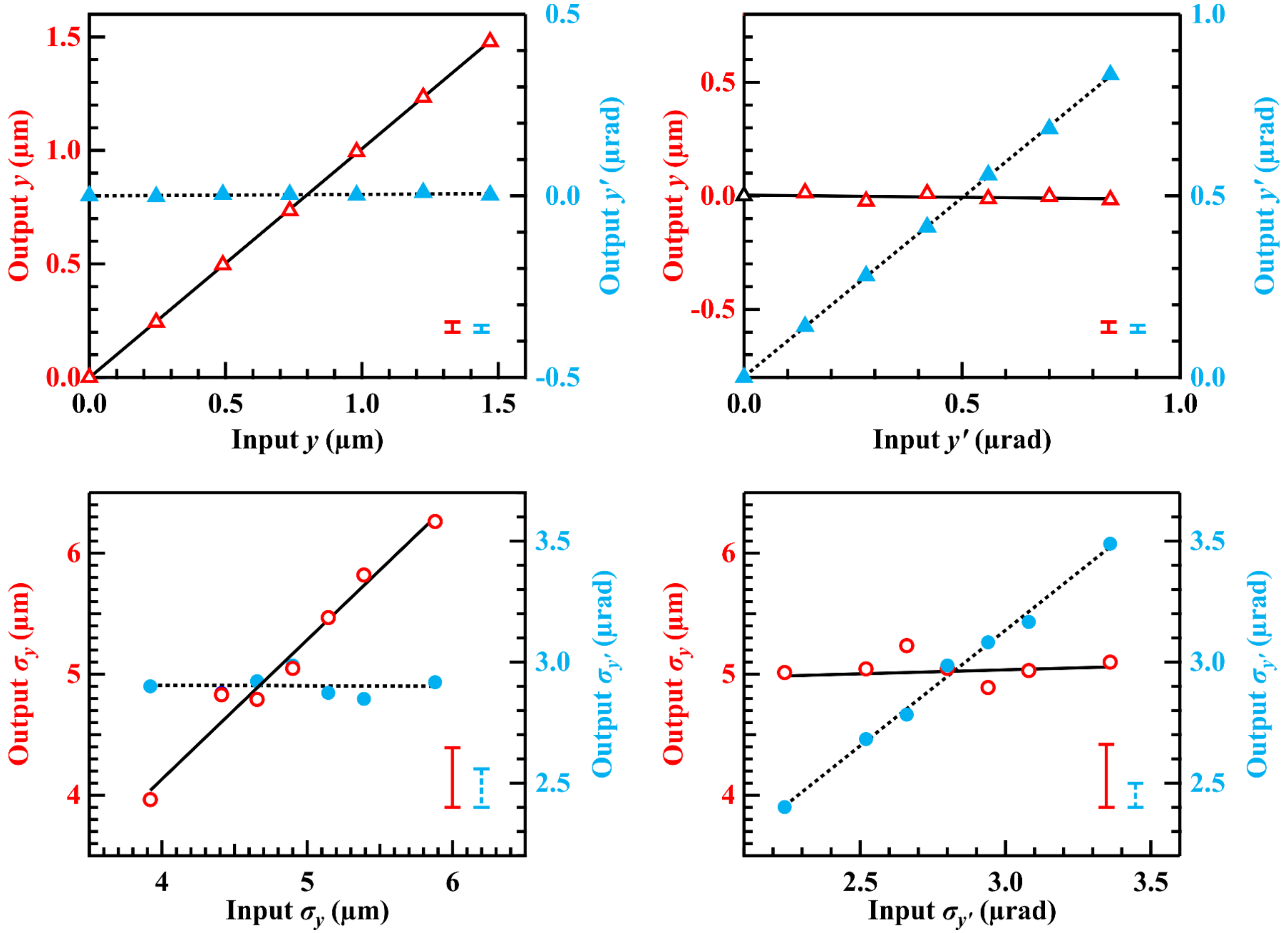

N. Samadi, X. Shi, and D. Chapman, J. Synchrotron Radiat. 26, 1863 (2019).

ps-BPM: optimization

- Resolution of the ps-BPM relies on photon flux and noise level (SNR)
- SNR determined by
  - Dark noise of the detector
  - Fluorescence from the K-edge filter
  - Compton scattering from the monochromator crystals
    - Single Bragg (SNR = 6700) at 6.6 m, detector at 10 m.
- Improve SNR by
  - Summing up N_h pixels in the horizontal direction: N_h=1000
  - Averaging over N_i images: N_i=8
  - Improve SNR by $\sqrt{N_h N_i}$
    - Single Bragg: SNR = 6×10^5

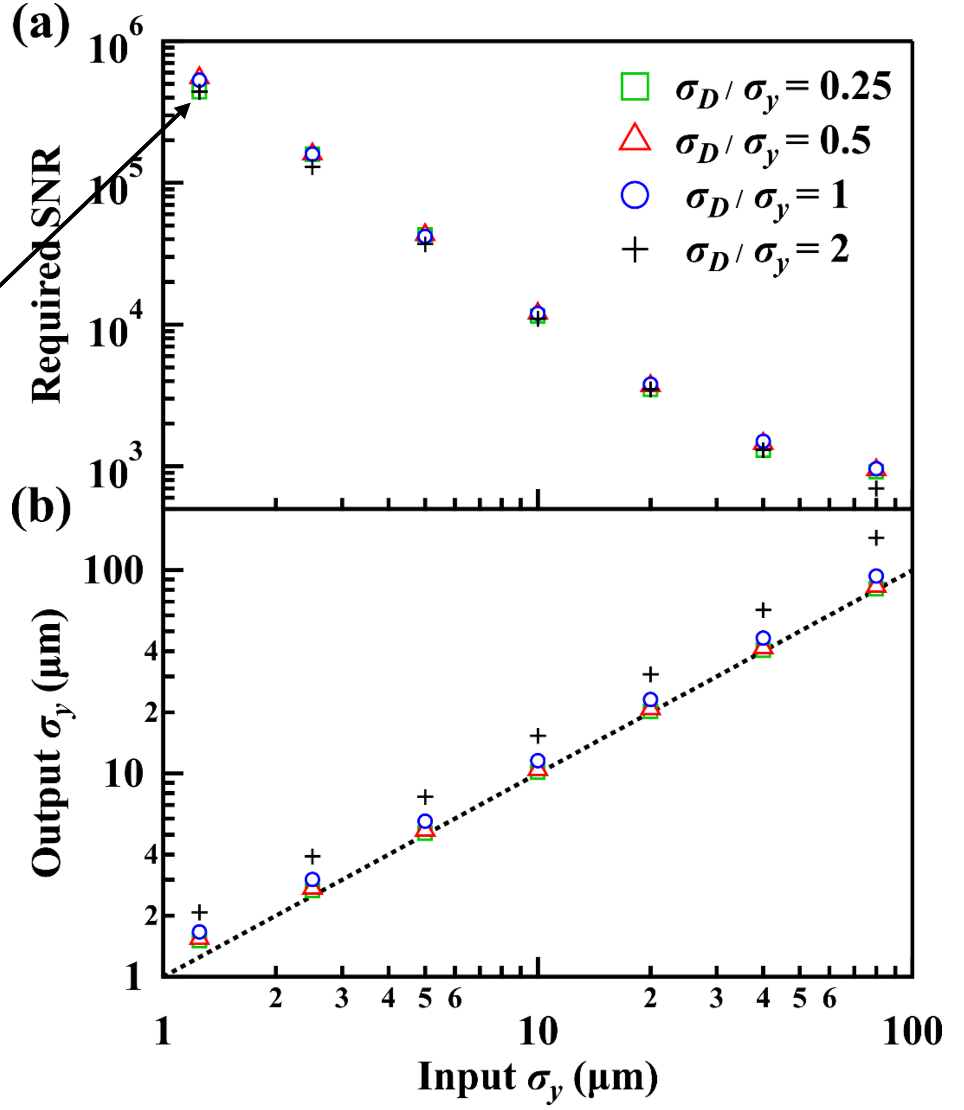

N. Samadi, X. Shi, L. Dallin, and D. Chapman, Phys. Rev. Accel. Beams 23, 024801 (2020).

Ps-BPM: summary

	Pinhole Imaging	Double Slit Interferometry	ps-BPM
Optical setup	Simple, aberration free	Require monochromator	Require monochromator
Measurement directions	All	1-D	1-D in mono diffraction plane
Fast measurement	Yes, white beam	No	yes y, y', not small σ_y, σ_y'
Resolution	Limited to >10 μm	Highest	High, but needs calibration
High-resolution detector	Yes	Yes	No
Optics fabrication	Hard	Hard	Easy
Information	Size and position	Size only	$y, y', \sigma_y, \sigma_y'$ simultaneously

Comparison of three methods (theory)

	Pinhole Imaging	Double Slit Interferometry	ps-BPM
Optical setup	Simple, aberration free	Require monochromator	Require monochromator
Measurement directions	All	1-D	1-D in mono diffraction plane
Fast measurement	Yes, white beam	No	yes y, y', not small σ_y, σ_y'
Resolution	Limited to >10 µm	Highest	High, but needs calibration
High-resolution detector	Yes	Yes	No
Optics fabrication	Hard	Hard	Easy
Information	Size and position	Size only	$y, y', \sigma_y, \sigma_y'$ simultaneously

Experimental comparison of three methods

- Electron source size measurement at the BMIT beamline at the Canadian Light Source

- Pinhole imaging
- Grating interferometry
- ps-BPM

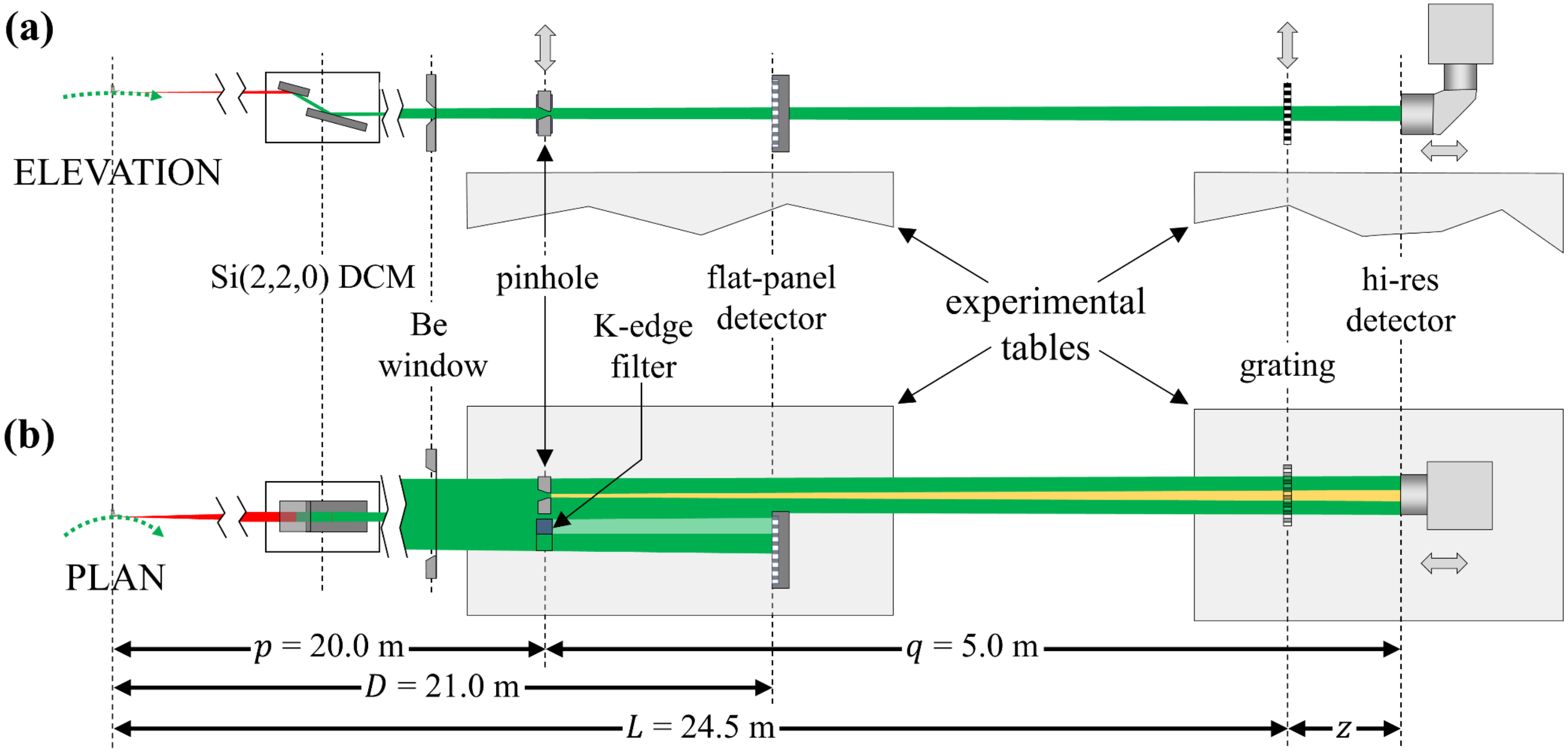

X. Shi, N. Samadi, L. Dallin, L. Assoufid, and D. Chapman, (2020) to be submitted.

Experimental comparison of three methods

- Pinhole imaging, 20 keV

$$\sigma^2_{\text{image},x,y} = M^2\sigma^2_{\text{source},x,y} + \sigma^2_{\text{pin}} + \sigma^2_{\text{det}}$$ → Neglected

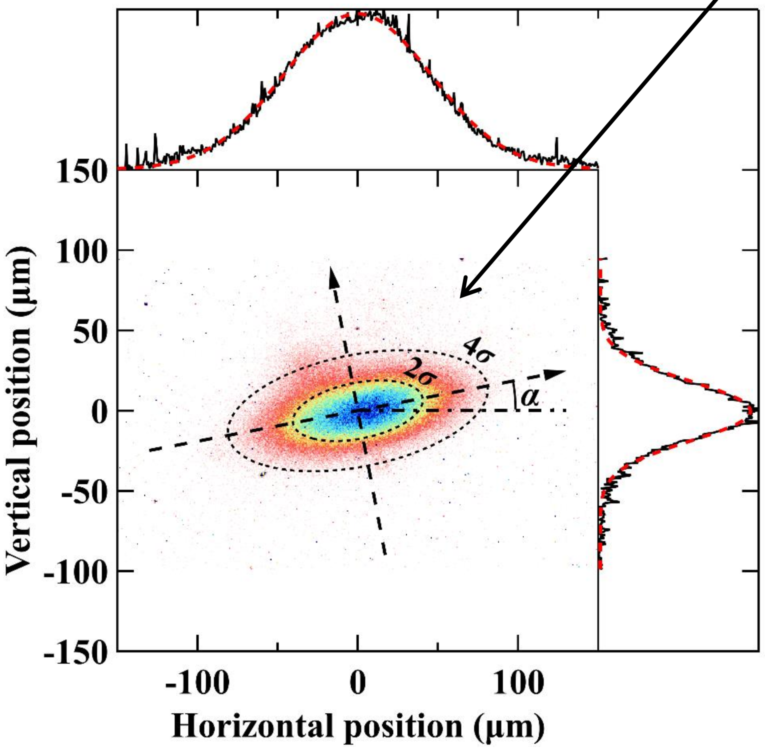

300 s acquisition time

$$I(x,y) = I_0 \exp\left[-\left(\frac{\cos^2\alpha}{2\sigma^2_{\text{image},x}} + \frac{\sin^2\alpha}{2\sigma^2_{\text{image},y}}\right)x^2 - \left(\frac{\sin 2\alpha}{4\sigma^2_{\text{image},x}} - \frac{\sin 2\alpha}{4\sigma^2_{\text{image},y}}\right)xy - \left(\frac{\sin^2\alpha}{2\sigma^2_{\text{image},x}} + \frac{\cos^2\alpha}{2\sigma^2_{\text{image},y}}\right)y^2\right]$$

$\sigma_{\text{source},x}$ (μm)	$\sigma_{\text{source},y}$ (μm)	α (°)
160±3	60±3	11.4±0.5

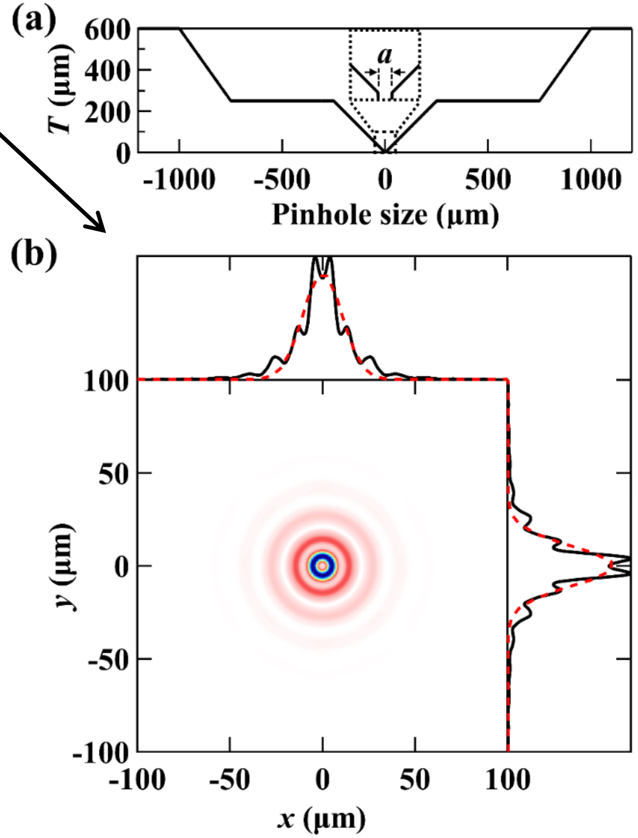

X. Shi, N. Samadi, L. Dallin, L. Assoufid, and D. Chapman, (2020) to be submitted.

Experimental comparison of three methods

- Grating interferometry, 20 keV

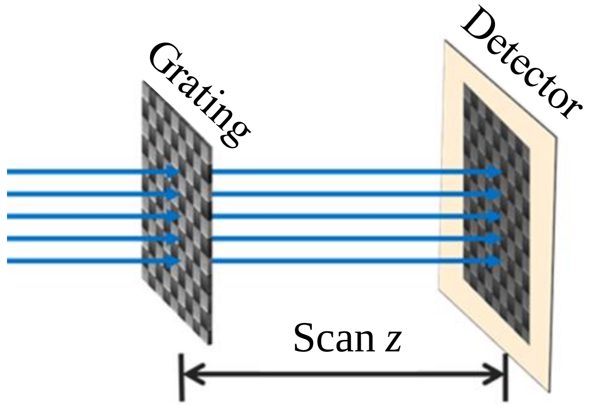

$$x = \frac{z\lambda}{p_x}$$

$$y = \frac{z\lambda}{p_y}$$

$$V_{x,y}(z) = A_{x,y} \left| \sin\left[\frac{\pi\lambda z L}{p_{x,y}^2 (L+z)}\right]\right| \exp\left[\frac{-2\pi^2 z^2 \Sigma_{source,x,y}^2}{p_{x,y}^2 (L+z)^2}\right]$$

$A_{x,y}$ — scaling parameter

$p_{x,y}$ — period of grating pattern

L — source-to-grating distance

$\Sigma_{source,x,y}$ — projected source size

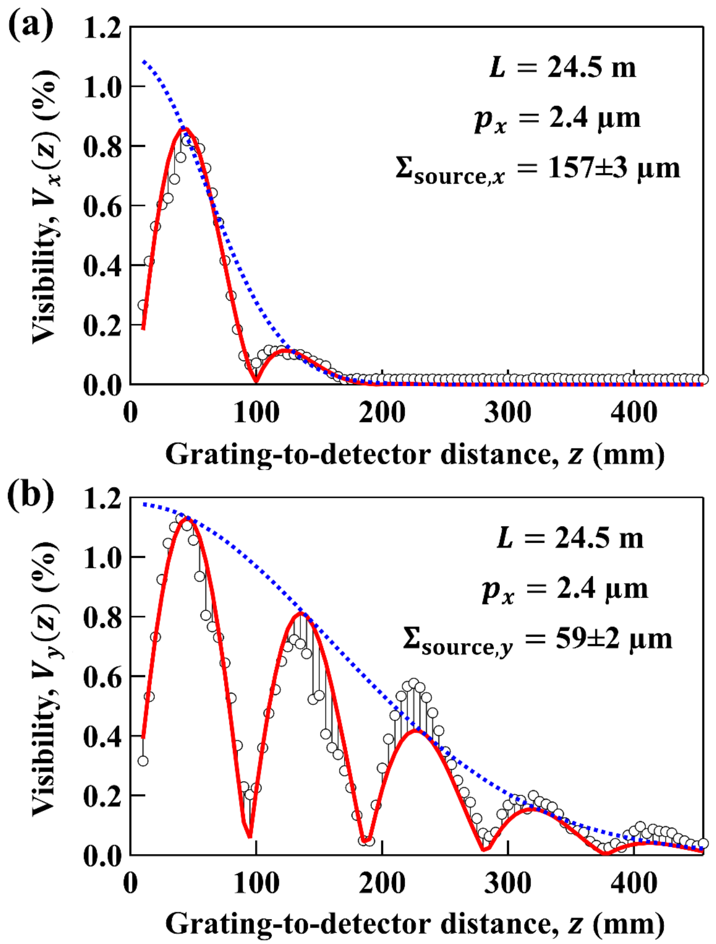

S. Marathe, X. Shi, M. J. Wojcik, N. G. Kujala, R. Divan, D. C. Mancini, A. T. Macrander, and L. Assoufid, Opt. Express **22**, 14041 (2014).

Technique	$\Sigma_{source,x}$ (µm)	$\Sigma_{source,y}$ (µm)
Grating	157 ± 3	59 ± 2
Pinhole	155 ± 3	61 ± 2

60 s per image, 2 hours total

X. Shi, N. Samadi, L. Dallin, L. Assoufid, and D. Chapman, (2020) to be submitted.

Experimental comparison of three methods

- ps-BPM calibration, Ba K-edge at 37.441 keV
  - σ_{IRF} is set to match $\Sigma_{source,y} = 60$ from pinhole and grating measurements

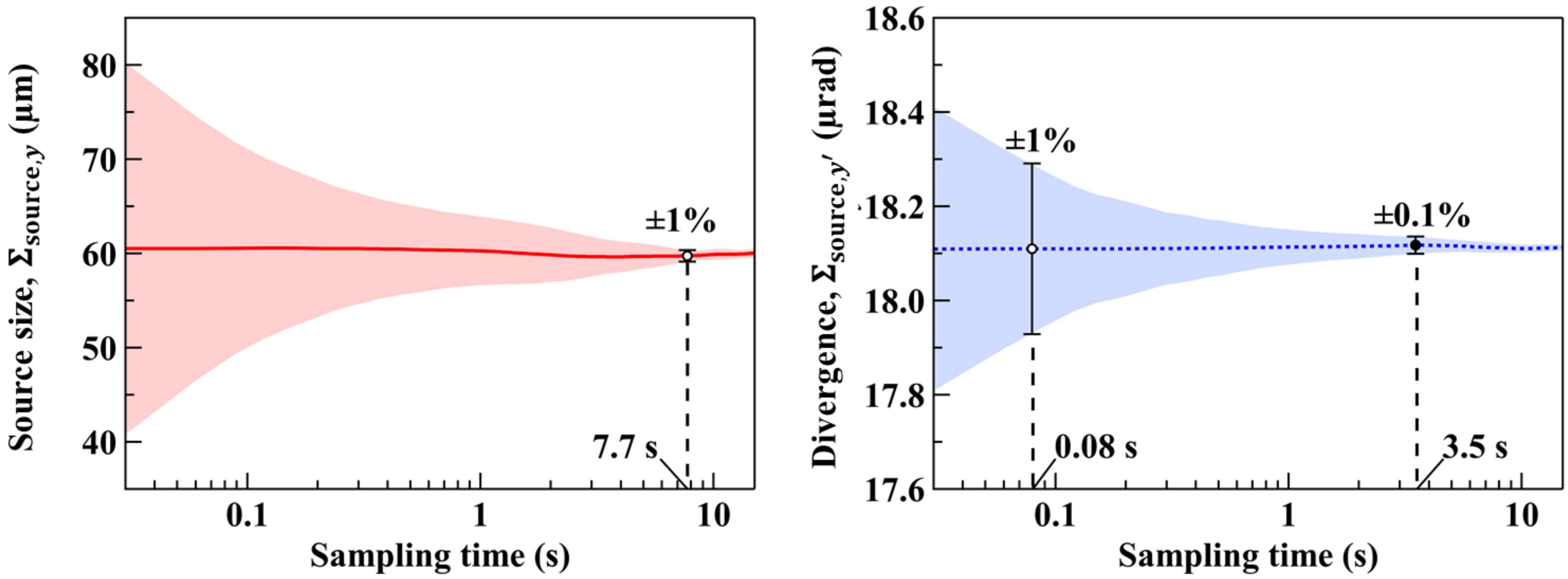

X. Shi, N. Samadi, L. Dallin, L. Assoufid, and D. Chapman, (2020) to be submitted.

Conclusion

- Three radiation-based methods for source size measurement were reviewed.
- They can provide complementary information.
  - Pinhole imaging provides 2-D imaging of the source.
  - Double-slit or grating interferometry provide high-resolution for measuring small source sizes
  - ps-BPM after calibration can provide real-time information on source position, angle, size, and divergence simultaneously.
- New facilities should consider combining multi-methods at a dedicated diagnostic beamline (normally bending magnet).
- Challenges:
  - ps-BPM works better at high energies while the other two methods prefer lower energies
  - Application to undulators and FELs
  - Studies are being carried out to solve these challenges.

Acknowledgment

PSI
Marco Stampanoni

University of Saskatchewan
George Belev

CLS
Rob Lamb
Mark Boland
Ward Wurtz
Bud Fugal
Denise Miller
Adam Webb
Arash Panahifar

APS
Louis Emery
Vadim Sajaev
Nick Sereno
Lahsen Assoufid
Albert Macrander

Thank you!